Photoelectrochemical study of Ta_3N_5 nanotubes for water splitting

2015 IOP Conf. Ser.: Mater. Sci. Eng. 97 012007

(http://iopscience.iop.org/1757-899X/97/1/012007)

Photoelectrochemical study of Ta_3N_5 nanotubes for water splitting

Sherdil Khan[1], Marcos J. Leite Santos *[2], Jairton Dupont [2], Sergio R. Teixeira*[1]

[1] Instituto de Física, Universidade Federal do Rio Grande do Sul, Av Bento Gonçalves 9500 POBox - 15051 CEP 91501-970, POA-RS, Brazil.
[2] Instituto de Química, Universidade Federal do Rio Grande do Sul, Av Bento Gonçalves 9500 POBox 15003, CEP 91501-970, POA-RS, Brazil.

E-mail address: *srgrbrtxr@gmail.com*

Abstract. Nanotubes (NTs) of Ta_3N_5 were synthesized by nitridation of Ta_2O_5 NTs. The samples were studied by scanning electron microscopy, UV-VIS spectrophotometry, x-ray diffraction and photoelectrochemical (PEC) measurements carried out in aqueous solutions of Na_2SO_4 and $Fe(CN)_6^{3-/4-}$. The results show the presence of trapping states on illuminated pristine Ta_3N_5 NTs in Na_2SO_4 (aq). These trapping states act as recombination center for photogenerated holes, affecting the photocatalytic performance of Ta_3N_5 NTs. On the other hand, by using $Fe(CN)_6^{3-/4-}$ (aq) the photogenerated holes were scavenged efficiently without giving rise to the trapping states at Ta_3N_5 NTs/solution interface. The results obtained by cyclic voltammetry, linear sweep voltammetry and electrochemical impedance spectroscopy have shown that the presence of these trapping states is a limiting step for water oxidation using pristine Ta_3N_5 NTs.

1. Introduction

Aiming to produce hydrogen from efficient solar-driven water splitting systems, many research groups have devoted their efforts to the study and development of photocatalysts [1,2, 3]. Several metal oxide semiconductors have been applied in photocatalytic and photoelectrochemical (PEC) water splitting, however most of these materials present large band gaps (> 3.0) absorbing light only within the ultraviolet region [4]. Once the visible spectrum accounts nearly half of the total energy from the sun that reaches the surface of the earth, the development of stable materials presenting absorption within the visible range is a key factor towards efficient water splitting systems. Within this context, Ta_3N_5 has emerged as a promising candidate, presenting adequate bandgap of ca. 2.1 eV and band edge at ca. 600 nm [5, 6]. According to the literature, the PEC water splitting performance of Ta_3N_5 is highly dependent on the loading of a suitable co-catalyst, while pristine Ta_3N_5 presents poor PEC activity [7]. Nevertheless, improved PEC activity from pristine Ta_3N_5 can be obtained by using a hole scavenging solution of $Fe(CN)_6^{3-/4-}$ [8]. In fact, the use of hole scavenging electrolytes such as Na_2SO_3, $Fe(CN)_6^{3-/4-}$, have resulted to improve PEC performance of other semiconductors [2,9].

The mechanism behind the poor PEC performance of pristine Ta_3N_5 based PEC devices, in water oxidation conditions, is not fully understood and a throughout study of the Ta_3N_5/electrolyte interface is necessary. Hence, in this work we have studied the PEC water splitting of Ta_3N_5 nanotubes. Firstly; we synthesized Ta_2O_5 NTs by modified anodization which helped us to preserve the tubular

morphology at high temperatures. Later, the precursor Ta_2O_5 NTs were transformed to Ta_3N_5 NTs by thermal treatment under ammonia environment. We have compared the PEC activity of Ta_3N_5 photoanodes under water oxidation conditions using Na_2SO_4 (aq) and hole scavenger oxidation using $Fe(CN)_6^{3-/4-}$(aq).

2. Experimental procedure

Ta (99.95%) sheet was cut into 2 cm × 2 cm small pieces, cleaned with acetone in ultrasound bath for 30 min, rinsed with water and dried under nitrogen flux. The anodization was performed in H_2SO_4 + 1 vol% of HF and 4 vol% of H_2O at 10°C during periods of 5 min and 20 min in a two electrode electrochemical cell. Ta disks were used as anode and Cu disks as cathode. The applied voltage was fixed to 50 V ramped by 10 V/s. Nitridation was performed at 800°C and 900°C (heating and cooling rate: 5°C/min) for 3 h under 100 ml/min of NH_3 flux. Photoelectrochemical measurements were performed separately in 0.1 M Na_2SO_4 (pH, 7.85), 0.1 M $K_4[Fe(CN)_6$ and 0.1 mM $K_3[Fe(CN)_6]$ (pH, 7.5). Ta_3N_5 NTs were used as working electrode, Pt wire as counter electrode and Ag/AgCl was used as a reference. The Ta_3N_5 NTs samples were characterized by scanning electron microscopy (SEM) performed in an EVO 50 from Zeiss, operated at 10 kV. Absorption spectra in the UV-Vis were obtained using a CARY 5000, Grazing angle X-ray diffraction (XRD) patterns were recorded by Shimadzu, Maxima XRD-7000 diffractometer with an incident angle of 0.3° with Cu K_α radiation (λ = 1.54 Å) at a 2θ range from 15° to 70° with a 0.05° step size and measuring time of 5s per step. Cyclic voltammetry (CV), Linear Sweep Voltammetry (LSV) and Electrochemical Impedance Spectroscopy (EIS) were performed by Auto-lab (AUT 84503) potentiostat. A Xe lamp (300W) was used as a source of electromagnetic radiation and an AM 1.5 filter was used, to obtain simulated solar spectrum. The light intensity was calibrated for 1 Sun conditions (100 mW.cm^{-2}), using a silicon photodiode.

3. Results and discussion

Fig. (1a, b) show the SEM images of the Ta_3N_5 NTs, displaying open top and closed bottom tubes. The as-anodized Ta_2O_5 NTs (not shown) were ca. 1.6 µm long, presenting wall thickness of 34 nm and outer diameter of 130 nm. In a previous study on Ta_2O_5 NTs prepared by anodization, we have found that anodization temperature controls the adherence of the NTs on the substrate. In addition to improve adherence, lowering the anodization temperature results in thicker walled nanotube [4].

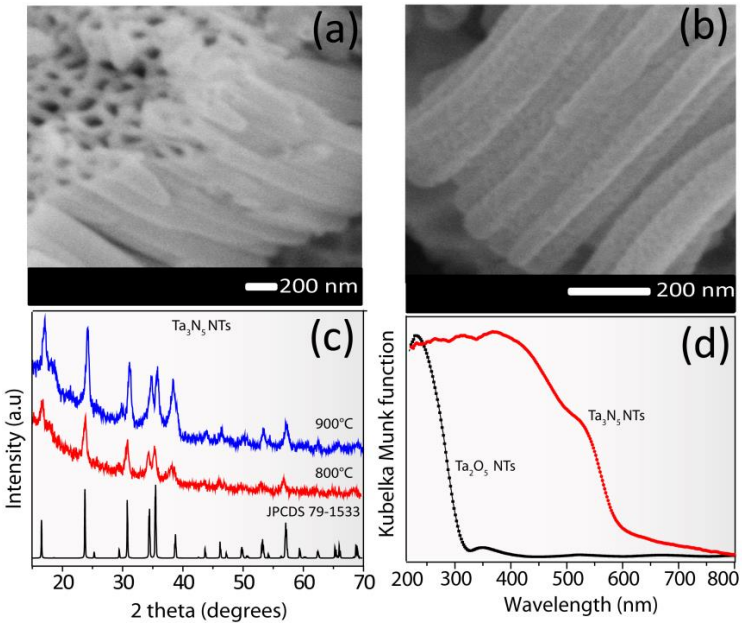

Fig. 1 SEM images of Ta_3N_5 NTs synthesized at (a) 800°C and (b) 900°C for 3 h. (c) XRD patterns of Ta_3N_5 NTs and (d) UV-Vis spectra of Ta_2O_5 and Ta_3N_5.

In this study, thick walled and well adhered Ta_2O_5 NTs were obtained at 10°C, making them preserve their morphology even when heated at 900°C. After nitridation at 800°C and 900°C, the length of the Ta_3N_5 NTs were reduced to ca 1.4 µm and 1.1 µm, respectively; compared to the length of the as-anodized NTs. In addition, slight decrease in the diameter of the NTs was observed. These changes in dimension are related to the density difference between the Ta_2O_5 and Ta_3N_5 structures [10]. Fig. 1c presents the grazing angle XRD patterns of the samples obtained by angle of incidence of 0.3°, with respect to the substrate surface. All peaks match with the orthorhombic phase of Ta_3N_5 (JPCDS file 79-1533). By using Rietveld Refinement technique, the average grain size of the nanotubes synthesized at 800°C and 900°C were 19.71, 43.51 nm respectively. Fig. 1d shows the absorption spectra of the as-anodized Ta_2O_5 and the Ta_3N_5 obtained at 800°C. After nitridation one can observe a large red-shift of the band edge from 320 nm (Ta_2O_5) to 600 nm (Ta_3N_5) and bandgap values of 3.9 and 2.1 eV respectively. In addition, the spectrum of Ta_3N_5 display a broad absorption mode above ca. 600 nm, which is related to ionic defects in the lattice resulting from the nitridation process [11].

In order to compare our findings to the literature, we have focused our study on the Ta_3N_5 samples obtained at 800°C [12]. Fig. (2a, b) display the cyclic voltammograms of the sample nitrided at 800°C for 3 h. The experiments were performed under dark (Fig. 2a) and under illumination (1 Sun) (Fig. 2b) in Na_2SO_4 (aq) electrolyte. For CV obtained under dark (Fig. 2a), as the potential is swept toward negative values, a strong increase of the capacitive current can be observed, starting from ca. −0.2V. Under cathodic applied potential the chemical capacitance associated with the electron population on the semiconductor begins to dominate the Helmholtz capacitance, where the quasi-Femi level gets closer to the conduction band which leads to a capacitive current [13]. The un-coordinated metallic ionic species that exist on the surface, will give rise to electronic states below the conduction band where capacitance is controlled by the Helmholtz region.

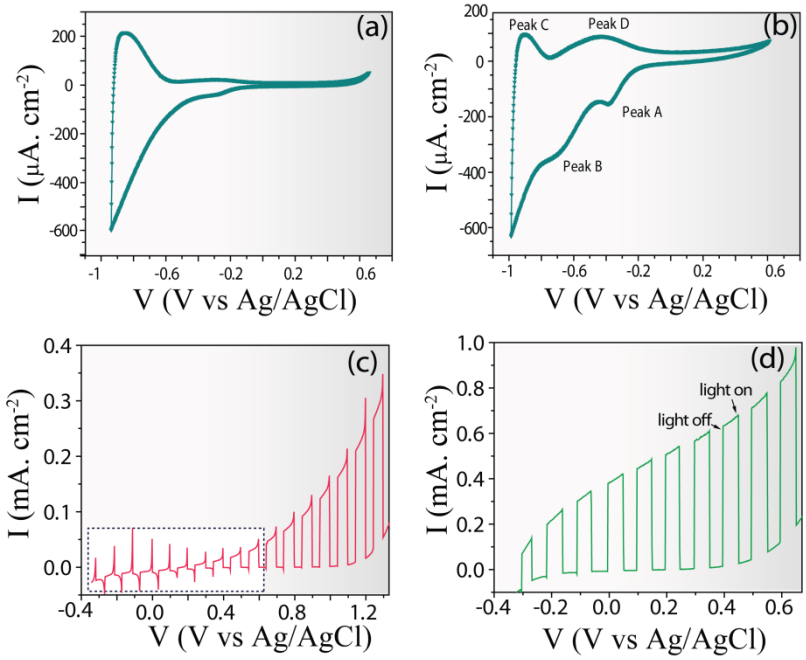

Fig. 2 CV curves of Ta_3N_5 NTs under (a) dark and (b) illumination. LSV curves of prisitine Ta_3N_5 NTs in aqueous electrolytes of (c) Na_2SO_4 and (d) $Fe(CN)_6^{3-/4-}$.

Considering the cathodic scan, under potentials more negative than −0.2 V vs Ag/AgCl, an exponential rise of the current is observed, which turned into an anodic peak at ca. −0.8 V, after the scan direction of the voltammetry is reversed from cathodic to anodic. The exponential increase in cathodic current gives rise to an exponential capacity, which is related to a charge

accumulation on the semiconductor [13]. Furthermore, from ca. −0.2 towards positive potentials a constant current can be observed. Nevertheless, whether the scan is anodic or cathodic the current in that potential window is constant. This behavior can be related to the carrier depletion on Ta_3N_5 NTs which is characteristic of the Mott-Shottky window. Fig. 2b displays the cyclic voltammetry curves of Ta_3N_5 NTs obtained under illumination (1 Sun). The exponential rise of current under negative potentials shown in Fig. 2a is transformed into peaks. For the pH used in the current study, the water reduction potential is −0.66V vs Ag/AgCl; therefore, the peak B which appears at ca. 0.7V vs Ag/AgCl and C are related to the redox process of water. An interesting feature of the CV under illumination is peak A appearing at ca. −0.3V vs Ag/AgCl, which cannot be related to any redox process of the electrolyte. Furthermore, upon returning the cathodic scan to the anodic direction a wider peak (peak D) appears. Similar features have been observed in the literature for hematite, where a sharp cathodic peak was related to the filling of narrow deep trapping states and broader anodic peak corresponded to relatively slow depopulation of these states [14].

In order to gain further insight on the role of trapping states, we have obtained LSV curves of pristine Ta_3N_5 NTs synthesized at 800°C during 3h. The experiments were performed at a scan rate of 10 mV/s, by chopping the light under a frequency of 0.2 Hz, using Na_2SO_4 (aq) Fe $(CN)_6^{3-/4-}$ (aq) redox couple Fig (2c, d). The PEC water splitting potential window where the solar to hydrogen efficiency can be obtained for Na_2SO_4 (aq) system is highlighted by black color dotted line in Fig. 2c. The photocurrent obtained in Fe $(CN)_6^{3-/4-}$ (aq) is clearly higher than in Na_2SO_4 (aq) for that potential window. Even when higher biasing is applied for Na_2SO_4 (aq) the photocurrent could not be improved as compared to Fe $(CN)_6^{3-/4-}$ (aq). In addition, the LSV curve of the system using $Fe(CN)_6^{3-/4-}$ (aq) redox couple presented better fill factor. In Na_2SO_4 (aq), at lower potentials, one can observe "overshoot" current spikes decaying momentarily and upon turning the light off sharp cathodic spikes are also observed. These results strongly suggest that under illumination, photogenerated holes reaching the Ta_3N_5 NTs surface in contact with Na_2SO_4 (aq), will be trapped and there will be large recombination of the photogenerated carriers. Once light is turn off, the holes which are trapped are oxidized resulting in a sharp cathodic peak. On the other hand, for higher applied potential biasing the cathodic spikes cannot be observed in Na_2SO_4. In these applied potentials the strong electric field at the double layer at the interface will force to neutralize the holes, as well as, it will separate the photogenerated charge carriers. These results clearly indicate that in order to obtain improved PEC performance from Ta_3N_5 NTs, the holes trapped on the surface are only neutralized by applying higher biasing potential. That is a major drawback, once the use of a large potential biasing will reduce the solar energy efficiency conversion for water splitting. Interestingly, the improved photocurrent and the absence of the cathodic spikes from Ta_3N_5 NTs in Fe $(CN)_6^{3-/4-}$ strongly suggests that the efficient hole scavenging nature of Fe $(CN)_6^{3-/4-}$ do not give rise to the trapping states.

To elucidate the mechanism of charge transfer across the Ta_3N_5 NTs/Na_2SO_4-interface, Nyquist plots were obtained at different applied potentials (Fig. 3a). Fig. 3a shows incomplete semicircles characteristic of a non-ideal capacitance behavior [15]. The data were fitted by an equivalent circuit shown in Fig. 3b [8]. The observed decrease in charge transfer resistance upon increasing the biasing potential, corroborates the earlier suggestion that; it is necessary to apply higher biasing to help to neutralize the trapping states. EIS corroborates these findings showing that for low charge transport resistance, higher biasing should be applied externally. In addition, from the observed decrease in charge transfer resistance upon increasing

the biasing potential; we may infer that the fill factor of Ta_3N_5 NTs in Na_2SO_4 (aq) would be poor which can clearly be seen in Fig. 2c.

For the analyses discussed above we have used Ta_3N_5 NTs obtained for 20 min of anodization and nitrided at 800°C for 3 hours. In order to investigate possible effect of the length of the NTs on the trapping states and to improve the photocurrent, we have decreased the length by anodizing the samples for only 5 min and further nitriding them at 800°C during 3 hours. The LSV curve obtained for this sample is shown in Fig. 3c (red color solid line).

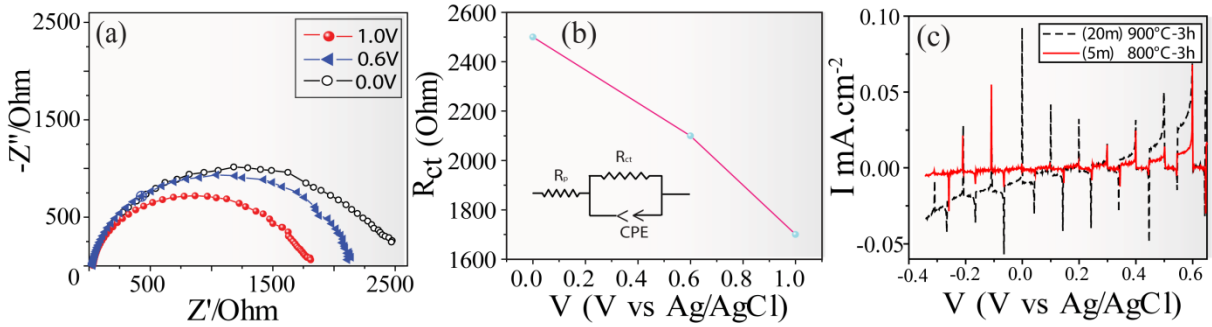

Fig.3 Nyquist plots of Ta_3N_5 NTs (a) and equivalent circuit fitting; charge transfer resistance R_{ct} vs applied potential (b). LSV curves of Ta_3N_5 NTs synthesized under two different conditions (c).

Comparing the photocurrent obtained from the sample with the longer length NTs (Fig. 2c, highlighted potential window), no improvement can be observed. Therefore, short length NTs, which are expected to present lower photogenerated charge carrier resistance, could not compete with the trapping states. To evaluate if the nanocrystallinity of the NTs may cope with the trapping states, we have obtained LSV curves of the sample anodized for 20 min and then nitrided at 900°C for the same period of 3 hours (Fig. 3c - black color dotted line). The cathodic and anodic spikes can be observed clearly. In addition, photocurrent is still not improved. Hence the trapping states are independent of the length and the crystallinity of pristineTa_3N_5 NTs. In the literature, the best PEC activity for Ta_3N_5 was observed by Domen´s group, once Ta_3N_5 was doped with Ba firstly; and then loaded with Co-Pi as a co-catalyst [7]. We may infer that the improvement observed in that report is related to avoiding the trapping states. Hence, we strongly suggest, to improve PEC performance of Ta_3N_5 NTs a similar kind of methodology should be followed.

4. Conclusions

In this work we have observed that photoelectrochemical activity of Ta_3N_5 NTs is highly dependent on the hole scavenging from the surface of the nanotubes. To improve water oxidation in Na_2SO_4 (aq) a higher applied potential is required, which is a major drawback to solar energy efficiency conversion of water splitting. On the other hand, due to the efficient hole scavenging ability of $Fe(CN)_6^{3-/4-}$ (aq), low biasing potential is required for Ta_3N_5 NTs that has presented an improved PEC performance once in this electrolyte no trapping state was observed.

Acknowledgements

The authors are grateful for financial support from the following Brazilian agencies: Conselho Nacional de Desenvolvimento Científico e Tecnológico (Processo: 477804/2011-0,

490221/2012-2 and 472243/2013-6) and Fundação de Amparo à Pesquisa do Estado do Rio Grande do Sul (FAPERGS – PqG 2011 Proc. 11/0837-0).

References

[1] Fernandes J A, Migowski P, Fabrim Z, Feil A F, Rosa G, Khan S, Machado G J, Fichtner P F P, Teixeira S R, Santos M J L and Dupont J 2014 TiO2 nanotubes sensitized with CdSe via RF magnetron sputtering for photoelectrochemical applications under visible light irradiation *Phys. Chem. Chem. Phys.*

[2] Klahr B, Gimenez S, Fabregat-Santiago F, Bisquert J and Hamann T W 2012 Electrochemical and photoelectrochemical investigation of water oxidation with hematite electrodes *Energ Environ Sci* **5** 7626.

[3] Goncalves R V, Migowski P, Wender H, Feil A F, Zapata M J M, Khan S, Bernardi F, Azevedo G M and Teixeira S R 2014 On the crystallization of Ta2O5 nanotubes: structural and local atomic properties investigated by EXAFS and XRD *Crystengcomm* **16** 797-804.

[4] Goncalves R V, Migowski P, Wender H, Eberhardt D, Weibel D E, Sonaglio F C, Zapata M J M, Dupont J, Feil A F and Teixeira S R 2012 Ta2O5 Nanotubes Obtained by Anodization: Effect of Thermal Treatment on the Photocatalytic Activity for Hydrogen Production *J. Phys. Chem. C* **116** 14022-30.

[5] Chun W-J, Ishikawa A, Fujisawa H, Takata T, Kondo J N, Hara M, Kawai M, Matsumoto Y and Domen K 2003 Conduction and Valence Band Positions of Ta2O5, TaON, and Ta3N5 by UPS and Electrochemical Methods *The Journal of Physical Chemistry B* **107** 1798-803.

[6] Moriya Y, Takata T and Domen K 2013 Recent Progress in the Development of (Oxy)nitride Photocatalysts for Water Splitting under Visible-Light Irradiation *Coordination Chemistry Reviews*.

[7] Li Y, Zhang L, Torres-Pardo A, Gonzalez-Calbet J M, Ma Y, Oleynikov P, Terasaki O, Asahina S, Shima M, Cha D, Zhao L, Takanabe K, Kubota J and Domen K 2013 Cobalt phosphate-modified barium-doped tantalum nitride nanorod photoanode with 1.5% solar energy conversion efficiency *Nature Communications* **4.**

[8] Kado Y, Lee C-Y, Lee K, Müller J, Moll M, Spiecker E and Schmuki P 2012 Enhanced water splitting activity of M-doped Ta3N5 (M = Na, K, Rb, Cs) *Chem Commun* **48** 8685.

[9] Zhang Q, Celorrio V, Bradley K, Eisner F, Cherns D, Yan W and Fermín D J 2014 Density of Deep Trap States in Oriented TiO2 Nanotube Arrays *The Journal of Physical Chemistry C* **118** 18207-13.

[10] Zhang Q H and Gao L 2004 Ta3N5 nanoparticles with enhanced photocatalytic efficiency under visible light irradiation *Langmuir* **20** 9821-7.

[11] Dabirian A and van de Krol R 2013 Resonant optical absorption and defect control in Ta3N5 photoanodes *Appl Phys Lett* **102.**

[12] Cong Y, Park H S, Wang S, Dang H X, Fan F-R F, Mullins C B and Bard A J 2012 Synthesis of Ta3N5 Nanotube Arrays Modified with Electrocatalysts for Photoelectrochemical Water Oxidation *J. Phys. Chem. C* **116** 14541-50.

[13] Bisquert J, Fabregat-Santiago F, Mora-Seró I, Garcia-Belmonte G, Barea E M and Palomares E 2008 A review of recent results on electrochemical determination of the density of electronic states of nanostructured metal-oxide semiconductors and organic hole conductors *Inorg. Chim. Acta* **361** 684-98.

[14] Bertoluzzi L, Badia-Bou L, Fabregat-Santiago F, Gimenez S and Bisquert J 2013 Interpretation of Cyclic Voltammetry Measurements of Thin Semiconductor Films for Solar Fuel Applications *J Phys Chem Lett* **4** 1334-9.

[15] Pajkossy T 1994 Impedance of rough capacitive electrodes *Journal of Electroanalytical Chemistry* **364** 111-25.